Interaction-induced nonlinear refractive-index reduction of gases in the midinfrared regime

K. Schuh, J. V. Moloney, and S. W. Koch

Phys. Rev. E **93**, 013208 — Published 21 January 2016

DOI: 10.1103/PhysRevE.93.013208

Interaction Induced Nonlinear Refractive Index Reduction of Gases in the Mid-Infrared Regime

K. Schuh* and J.V. Moloney
Arizona Center for Mathematical Sciences, Department of Mathematics, University of Arizona, Tucson, Arizona 85721, USA and College of Optical Sciences, University of Arizona, Tucson, Arizona 85721, USA

S.W. Koch
College of Optical Sciences, University of Arizona, Tucson, Arizona 85721, USA and Department of Physics and Material Science Center, Philipps-University, 35032 Marburg, Germany

The nonlinear optical response of a dilute atomic gas to ultra-short high-intensity mid-infrared pulse excitation is calculated fully microscopically. The optically induced polarization dynamics is evaluated for the interacting many-electron system in a gas of hydrogen atoms. It is shown that the many-body effects during the excitation distinctly influence not only the atomic ionization dynamics, but also the nonlinear polarization response in the mid-infrared regime. The delicate balance between the Kerr focusing and the ionization induced defocussing is dramatically modified and a significant decrease of the nonlinear refractive index is predicted for increasing wavelength of the exciting pulse.

PACS numbers: 52.20.Fs, 42.65.-k, 42.65.Hw

I. INTRODUCTION

In recent years, the scientific attention towards strongly nonlinear propagation dynamics of high-intensity pulses in air or other dilute gases has expanded into the mid-infrared regime [1–7]. Shifting the wavelength from the optical into the mid-infrared range strongly modifies the importance of the contributing physical phenomena and the relevant dispersive properties. In particular, the interplay between the focusing nature of the Kerr effect and the counteracting defocusing caused by the nonlinear polarization contribution of liberated electrons governs the spatio-temporal evolution of the light pulses. One important aspect in the theoretical modeling is therefore the consistent evaluation of the atomic or molecular ionization dynamics. In the past, most of the calculations involved the numerical solution of the time dependent Schrödinger equation [8, 9], using S-matrix theory [10] or the Keldysh-Faisal-Reiss [11–13] strong-field approximation [14, 15]. Besides the technical differences between these approaches, they all describe the ionization dynamics at the single-atom level, i.e., they do not consider the many-body interaction effects due to the presence of multiple atoms or molecules allowing for various scattering processes of the continuum-state electrons.

In our fully microscopic studies of atomic ionization due to strong-field optical excitation[16], we have shown that the Coulombic collisions of the excited-state electrons with other electrons, with ions, and with neutrals leads to an increased ionization. In particular, we found that the difference of the ionization degree relative to a non-interacting model calculation can reach multiple orders of magnitude for excitation intensities below the ionization threshold. Whereas this increase does not cause a substantial change of the polarization response at optical frequencies, it is known that the polarizability of free electrons increases quadratically with the wavelength of the exciting field causing a stronger polarization response in the mid-infrared regime. Hence, we can expect significant changes of the nonlinearities with increasing excitation wavelengths.

To quantitatively investigate these effects, we extended our microscopic model calculations into the long-wavelength domain. As the most important result, we find large changes in the nonlinear refractive index in the mid-infrared regime ($\lambda > 3\mu$m) caused by the interaction induced ionization increase. As a consequence, we predict significant modifications in the interplay between the Kerr focusing and the plasma induced defocusing important for the propagation of high intensity pulses and the generation of ionized filaments [17] which displays a rich field of interesting physical phenomena and applications like remote sensing [18], white light [19] and THz generation [20], pulse compression [21], and lightening guiding [22].

II. MODEL

In order to microscopically compute the nonlinear refractive index variations as function of the exciting pulse properties, we consider the simple system of a dilute hydrogen gas where we include only the hydrogen ground state (s) and the ionized continuum states classified by the carrier momentum $\vec{k}$. We adopt the semiclassical approach where the strong optical field is treated clas-

* kschuh@optics.arizona.edu

sically while the atomic gas is described quantum mechanically. The optical transitions are evaluated in the dipole approximation using a generalized version of the Optical Bloch Equations [23, 24] which allow for the self-consistent analysis of the light-atom and the Coulombic many-body interactions.

A. Optical Bloch Equations

For our simple hydrogenic model system, we can derive the coupled equations for the ground-state population f_s, the continuum-state populations $f_{\vec{k}}$, and for the microscopic polarization $P_{s\vec{k}}$ between bound and continuum states, as well as the continuum-continuum-state polarization $P_{\vec{k}\vec{k}'}$ by evaluating the respective Heisenberg equations of motion for the relevant operator combinations[23, 24]. As shown in Ref. [25], we obtain the dynamic equations

$$i\hbar\frac{d}{dt}f_s = \sum_{\vec{k}}\Omega^*_{s\vec{k}}P^*_{s\vec{k}} - \Omega_{s\vec{k}}P_{s\vec{k}} \tag{1}$$

$$i\hbar\frac{d}{dt}f_{\vec{k}} = N\left[\Omega_{s\vec{k}}P_{s\vec{k}} - \Omega^*_{s\vec{k}}P^*_{s\vec{k}}\right] - \tfrac{e}{\hbar}\vec{\nabla}_{\vec{k}}f_{\vec{k}}\vec{E} \tag{2}$$

$$\begin{aligned} i\hbar\frac{d}{dt}P_{s\vec{k}} = {} & \left[\epsilon_s - \epsilon_{\vec{k}}\right]P_{s\vec{k}} + \Omega^*_{s\vec{k}}\left[f_{\vec{k}} - f_s\right] \\ & - \tfrac{e}{\hbar}\vec{\nabla}_{\vec{k}}P_{s\vec{k}}\vec{E} + \textstyle\sum_{\vec{k}'\neq\vec{k}}\Omega^*_{s\vec{k}'}P_{\vec{k}'\vec{k}} \\ & + i\hbar\tfrac{d}{dt}P_{s\vec{k}}|_{\text{e-e}} \end{aligned} \tag{3}$$

$$\begin{aligned} i\hbar\frac{d}{dt}P_{\vec{k}\vec{k}'} = {} & \left[\epsilon_{\vec{k}} - \epsilon_{\vec{k}'}\right]P_{\vec{k}\vec{k}'} - \tfrac{e}{\hbar}\vec{\nabla}_{\vec{k}}P_{\vec{k}\vec{k}'}\vec{E} \\ & + \Omega_{s\vec{k}}P_{s\vec{k}'} - \Omega^*_{s\vec{k}'}P^*_{s\vec{k}}\,, \end{aligned} \tag{4}$$

where $\frac{d}{dt}P_{s\vec{k}}|_{\text{e-e}}$ is the many-body part discussed later and the rest of the equations describes the optical single-particle part. Here, N is the number of atoms, ϵ_s is the ground-state energy of the $1s$-state, whereas the energy of the free electrons follows a parabolic dispersion $\epsilon_{\vec{k}} = \frac{\hbar^2\vec{k}^2}{2m}$ with the electron mass m. The Rabi frequency $\Omega_{s\vec{k}}(t) = \vec{d}_{s\vec{k}}\vec{E}(t)$ is the product of the linear polarized E-field $\vec{E}$ and the dipole matrix elements $\vec{d}_{s\vec{k}} = <s|-e\vec{r}|\vec{k}>$ with the elementary charge e.

Equations (1) - (4) constitute a system of coupled Bloch equations describing the transitions between the groundstate s and the continuum states $\vec{k}$ of hydrogen. Whereas the qualitative features of the calculated results for this relatively simple model should be representative for more realistic systems, there are quantitative differences. For example, the Kerr coefficient of our simple hydrogen model is about 5-fold smaller than the coefficients of N_2 and O_2 as given in Ref. [26], while the optical transition strength is about 7-fold smaller than the strength of N_2 and O_2 as calculated from pseudospectral lines obtained from Ref. [27].

B. Many-Body Effects

Considering the different Coulomb interaction processes in a strong-pulse non-resonantly excited atomic gas, we showed in our previous work [16] that the ionization is mainly influenced by the excitation induced dephasing (EID) of the coherent polarization due to the interaction between the continuum-sate electrons. The electron-ion and electron-neutral scatterings provide only very small corrections such that it is well justified to restrict the many-body aspects of our current investigations to the electron-electron EID.

In Ref. [25], we evaluate the EID contributions at the level of the second-Born Markov approximation, omitting all memory effects. Using this approximation to compute the nonlinear optical response in the long-wavelength regime, we obtained unrealistically large changes relative to those of free-particle calculations. Hence, we have to systematically improve our microscopic analysis, i.e. we have to include non-Markovian features in the interaction dynamics. For this purpose, we compute the EID contribution using the nonequilibrium Greens functions method.[28, 29]

In the most general form, we would have to deal with two-time Greens functions obeying numerically extremely demanding equations. However, it has been shown that efficient approximations[28] can be employed that render this approach more practical. A first simplification is obtained by applying the generalized Kadanoff-Baym ansatz [29], which reduces the problem to one-time quantities, i.e. occupations f and polarizations P. In the fully retarded variant, this ansatz includes memory effects taking the non-instantaneous nature of the interactions into account.

This way, we obtain from the Kadanoff-Baym equation [28] in the low density limit $(1-f=1)$ the dynamic equation for the many-body part of the polarization evolution

$$\frac{d}{dt}P_{s\vec{k}}|_{\text{e-e}} = -\hbar^2\int_{t_0}^{t}dt'\sum_{\vec{k}',\vec{q}}W_q(t)W^*_q(t')G^{R,*}_s(t,t')G^{R}_{\vec{k}+\vec{q}}(t,t')G^{R,*}_{\vec{k}}(t,t')G^{R}_{\vec{k}'-\vec{q}}(t,t')P_{s\vec{k}}(t')f_{\vec{k}'}(t') \quad . \tag{5}$$

Here,

$$W_q(t) = \frac{1}{V}\frac{e^2}{\epsilon_0(q^2+\kappa^2(t))} \tag{6}$$

is the screened Coulomb potential with the permittivity ϵ_0, the time-dependent inverse screening length κ, the system volume V and $q = |\vec{q}|$. Since we are dealing with

a highly diluted atomic gas, it is justified to treat the Coulomb screening within the Debye-Hückel approximation [23]. Then, the retarded Green's functions are given by

$$G^R_{\vec{k}}(t,t') = \frac{1}{\mathrm{i}\hbar} e^{\int_{t'}^{t} dt'' \frac{1}{\mathrm{i}\hbar}\epsilon_{\vec{k}} - \Gamma_{\vec{k}}(t'')} \ . \tag{7}$$

The imaginary part of the exponent with the energy $\epsilon_{\vec{k}}$ ensures the overall energy conservation and the real part describes the memory decay with the rate Γ due to the transition of electrons out of the considered state. In the investigated system, the dominant contribution to this decay is given by optical transitions from the continuum states into the ground state as described by Eqs. (1) - (4). Limiting our calculation to this contribution, we approximate the decay rate by

$$\Gamma(t) = \begin{cases} -\frac{\sum_{\vec{k}} \frac{d}{dt} f_{\vec{k}}}{\sum_{\vec{k}} f_{\vec{k}}} & \text{if} \quad \sum_{\vec{k}} \frac{d}{dt} f_{\vec{k}} < 0 \\ 0 \end{cases} \tag{8}$$

assuming a uniform rate Γ for all k. Our earlier studies[25] showed that for the considered strongly off-resonant excitation conditions the continuum-state occupations adiabatically follow the square of the exciting field as long as there is no significant ionization. Therefore, the transiently excited electrons are returned to the groundstate within an optical half cycle, which therefore sets an upper limit for the memory depth, i.e., the time interval contributing to the time integration in Eq. 5. Since the adiabatic following of the continuum-state occupations is independent of the intermediate states, these states have no significant influence on the EID effects in the low ionization regime.

III. NUMERICAL EVALUATION

We numerically evaluate Eqs. (1) - (5) for our model hydrogen gas. Unless noted otherwise, we assume ambient pressure, an unexcited system before the pulse arrives, and a $\cos^2$-envelope with a full-width at half-maximum of 100 fs. We neglect impact ionization effects since the pertinent cross sections are smaller than $0.01\mathrm{nm}^2$ [30] such that even at longer wavelengths the avalanche ionization is significantly smaller than the many-body induced ionization.

In Fig.1, we show the computed ionization degree for pulses with wavelengths of 1 and 10 μm with (red, dashed) and without (blue, continuous) electron interaction induced dephasing. In the non-interacting case, the ionization exhibits a sharp threshold behavior with a fast increase around 1e18 $\mathrm{W/m}^2$ for our model hydrogen system. We note that the many-body effects influence the ionization degree mostly in the regime of lower intensities below this threshold, whereas the differences between interacting and non-interacting system gradually disappear for higher intensities. See Ref. [16] for an extended discussion.

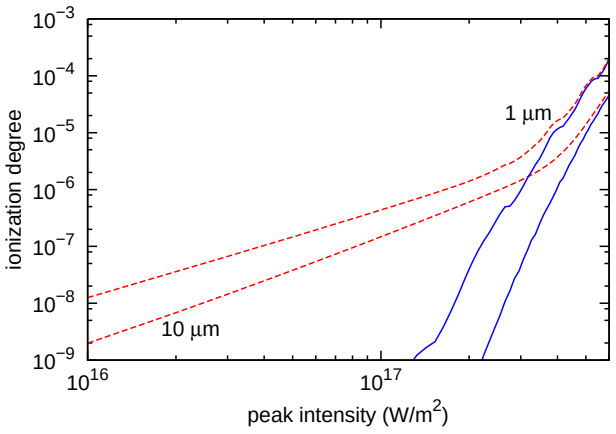

FIG. 1. (color online) Ionization degree at the end of 100 fs pulses with 1 and 10 μm central wavelength with (red, dashed) and without (blue, continuous) many-body effects. The Coulomb interaction significantly increases the ionization degree below the threshold for optically induced ionization around 1e18 $\mathrm{W/m}^2$.

The dominant contributions to the nonlinear refractive index originate from the Kerr effect on the one hand and the electronic polarization on the other hand. According to Ref. [31], the frequency dependency of the Kerr part in the long wavelength limit can be approximated as

$$n_{\mathrm{Kerr}}(\omega) \propto 1 + 2\frac{\omega^2}{\omega_i^2} \tag{9}$$

where ω_i is an effective ionization energy. Hence, the Kerr part decreases slowly with increasing wavelength. In contrast, the magnitude of the contributions from the free electrons

$$n_{\mathrm{e}}(\omega) \propto -\frac{1}{\omega^2} \tag{10}$$

increases quadratically with the wavelength. Thus, the electron part becomes increasingly more important for longer wavelength excitation.

In our microscopic model, the polarization density

$$\begin{aligned} p(t) = \quad & \tfrac{N}{V} \textstyle\sum_k 2\Re P_{sk}(t) d^*_{sk} \\ & + \int_{t_0}^{t} dt' \ \tfrac{1}{V} \textstyle\sum_k f_k(t') k \tfrac{e\hbar}{m} \end{aligned} \tag{11}$$

is calculated from the occupations of the excited continuum states f_k and the microscopic polarizations P_{sk}. The nonlinear polarization is obtained by subtracting the linear part from the full polarization where the linear part is extrapolated from a low intensity calculation. In order to study the interplay between the Kerr and the liberated electron contributions, we introduce an effective instantaneous nonlinear refractive index

$$n_{\mathrm{NL}}(t) = \frac{P_c^{\mathrm{NL}}(t)}{2\epsilon_0 E_c(t)} \tag{12}$$

where $P_c^{\mathrm{NL}}(t)$ and $E_c(t)$ are the frequency components at the carrier frequency of the nonlinear polarization density

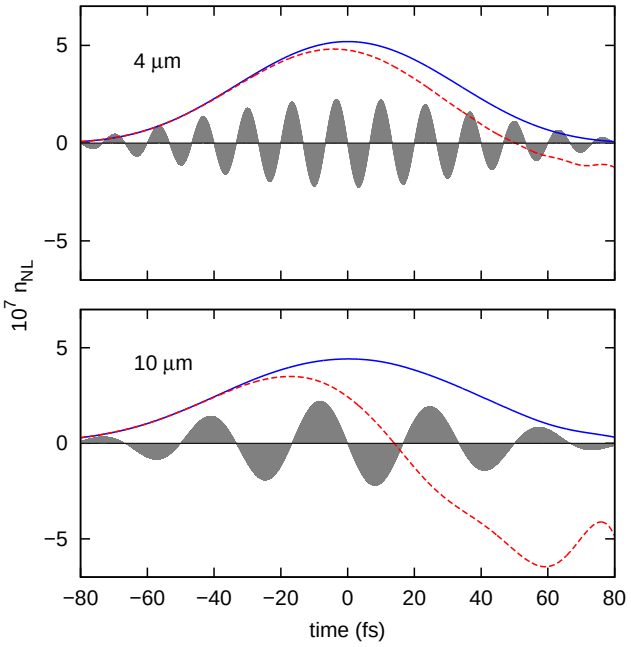

FIG. 2. (color online) Time-evolution of the nonlinear refractive index with (red, dashed) and without (blue, continuous) many-body effects during the excitation of the system with a pulse of 4 μm (upper frame) or 10 μm (lower frame) central wavelength. The intensity is 1.4e17 W/m^2. At the beginning of the pulses, i.e. in the absence of liberated electrons, the nonlinear refractive index increases linearly with the intensity (Kerr effect) and there is no noticeable change due to the many-body effects. Gradually, the EID effects lead to an increasing ionization causing a reduction of the nonlinear refractive index at later times during the pulse. Due to the larger polarizability of the liberated electrons at longer wavelengths, this effect is stronger at longer wavelengths.

$p_{\rm NL}$ and the E-field, respectively. These two values are obtained by a Fourier transformation of $p_{\rm NL}$ and E with a Gaussian shaped filter centered at time t and a FWHM of about $\frac{6}{\omega}$.

The time evolution of $n_{\rm NL}(t)$ during the excitation with pulses of 4 μm (upper frame) and 10 μm (lower frame) central wavelength are shown in Fig. 2. The chosen intensity of 1.4e17 W/m^2 is below the optical ionization threshold such that the Coulomb induced dephasing dominates the ionization dynamics. Without EID (blue solid lines) the nonlinear refractive index follows the square of the E-field envelope signifying the dominance of the Kerr effect. Accordingly, the nonlinear refractive index increases linearly with the peak intensity of the pulses.

In the case of the 4 μm pulse, the effects of the EID increased ionization (red dashed line) are small, leading only to a minor decrease of the refractive index during the second half of the pulse. However, since the susceptibility of the liberated electrons depends quadratically on the wavelength, the same intensity pulse with a 10μm central wavelength experiences much larger effects due to the EID increased ionization.

While there is no ionization at the beginning of the pulse and thus no difference between the case with and without EID, the EID increased ionization during the pulse causes an increasingly larger electronic contribution to the nonlinear index. Hence, in comparison to the non-interacting case, where virtually no ionization is present at this intensity, the instantaneous n_{NL} decreases. For later times, n_{NL} becomes negative showing that the Kerr effect is more than compensated by the polarization contribution of the liberated electrons.

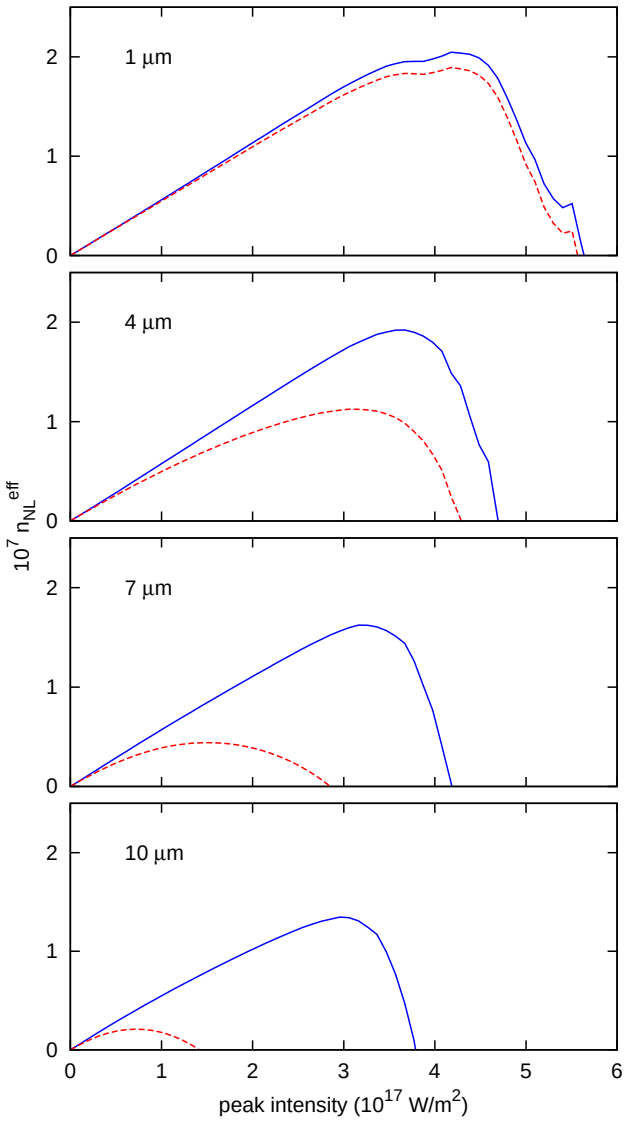

FIG. 3. (color online) Effective nonlinear refractive index $n_{\rm NL}^{\rm eff}$ with (red, dashed) and without (blue, continuous) many-body effects for different wavelengths. Due to the EID increased ionization, the intensities necessary for a compensation of the Kerr effect by free electrons is significantly reduced at longer wavelengths.

In order to compare a broad range of pulses, we evaluate the effective pulse-integrated nonlinear refractive index $n_{\rm NL}^{\rm eff} = P_c^{\rm NL}/(2\epsilon_0 E_c)$, where $P_c^{\rm NL}$ and E_c are the components of the nonlinear polarization and the E-field at the carrier wavelength, respectively. The resulting $n_{\rm NL}^{\rm eff}$ as function of peak intensity is depicted in Fig. 3 for different wavelengths with (red, dashed) and without (blue, continuous) the inclusion of EID effects. As discussed above, the ionization degree without EID is negligibly small until it increases rapidly at the optical ionization threshold. Thus, the Kerr effect dominates in that regime and causes a linear increase of $n_{\rm NL}^{\rm eff}$. As soon as the optical ionization threshold is reached, the contribution of the liberated electrons becomes rapidly dominant causing $n_{\rm NL}^{\rm eff}$ to decrease and eventually turn negative.

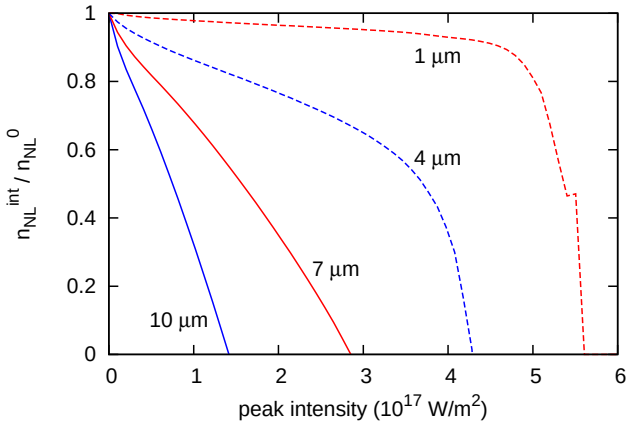

FIG. 4. (color online) Ratio between the effective nonlinear refractive index with and without EID effects for the same pulses as in Fig. 3.

The presence of EID drastically changes the ionization behavior below the optical ionization threshold and therefore the polarization response at longer wavelengths. Fig. 4 shows the relative change in the nonlinear refractive index due to the EID effects. While this change is rather small at 1 μm, there are significant modifications at longer wavelengths due to the increased polarizability of the liberated electrons.

Most notable in Fig. 3, the original Kerr regime with linearly increasing nonlinear index is changed by the EID into a sublinear increase followed by a roll over and decrease towards negative values. Moreover, both the maximum positive value of $n_{\rm NL}^{\rm eff}$ and the critical intensity where Kerr and free electron contributions cancel each other decrease with increasing wavelength.

One interesting aspect of the EID induced effects is their dependence on the particle density, i.e. the gas pressure. Single particle effects increase linearly with the pressure in contrast to the nonlinear variation of the many-body effects resulting from the interaction between different particles. In particular, the effect of electron-electron collisions scales quadratically with the density as long as phase-space filling is not important.

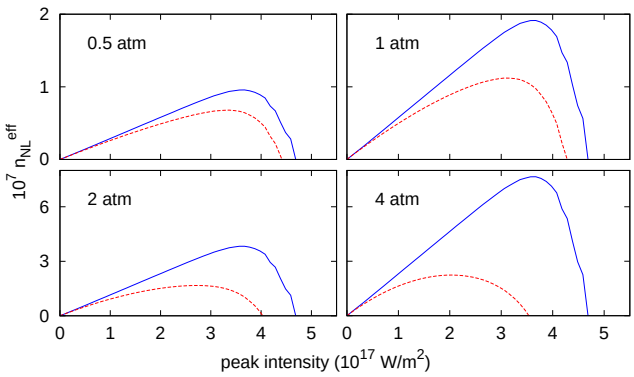

FIG. 5. Effective nonlinear refractive index $n_{\rm NL}^{\rm eff}$ with (red, dashed) and without (blue, continuous) EID effects for 100 fs, 4 μm pulses at different pressures (see labels, the scales for $n_{\rm NL}^{\rm eff}$ vary between the upper and lower graphs by a factor of 4). While the index depends linearly on the pressure in the non-interacting atom model, this pressure dependence becomes much weaker in the presence of EID.

To illustrate this density dependence, we show in Fig. 5 the effective nonlinear refractive index as function of intensity for different pressures. As expected, the single particle calculations (blue, continuous) predict a linear increase with the pressure. In contrast, the calculations with EID (red, dashed) show a much weaker increase for lower intensities, a faster decrease at higher intensities, and a reduction of the critical intensity where the effective nonlinear refractive index becomes negative.

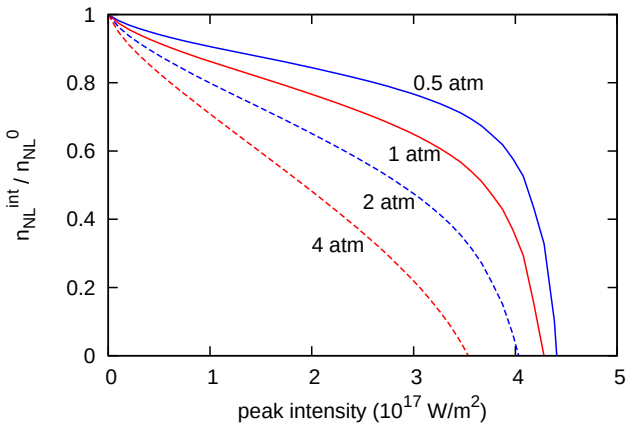

FIG. 6. Ratio between the effective nonlinear refractive index with and without many-body effects for the same pulses as in Fig. 5: The increasing many-body interaction causes a faster reduction of the nonlinear refractive index with increasing pressure.

The increasing impact of the EID induced effects with increasing pressure shows up clearly when we look at the ratio between the effective nonlinear refractive index with and without EID as shown in Fig. 6. We clearly notice

a much more rapid decrease of this ratio with increasing pressure caused by the nonlinear density dependence of the EID effects.

IV. DISCUSSION AND CONCLUSION

In summary, we present a comprehensive model study of the influence of excitation-induced dephasing effects on the nonlinear response of gases in the mid-infrared regime. Our results show that the ionization degree at intensities below the optical ionization threshold is dominated by electron-electron many-body interactions and increases roughly quadratically with intensity. Whereas the still rather low ionization degree below the optical threshold has a relatively small impact on the polarization response of optical pulses, they significantly change the response in the mid-infrared regime due to the larger polarizability of the liberated electrons. Since a positive (negative) value of the nonlinear index contributes to self focussing (defocussing), the computed modifications, in particular the predicted lower values of the critical intensities for the sign change and the reduced maximal index values should be of great importance for propagation problems at these longer wavelengths.

Several of the computed features should be accessible in experiments. For example, the pressure dependence of $n_{\mathrm{NL}}^{\mathrm{eff}}$ as shown in Fig. 5, in particular the significantly slower than linear increase of the maximum of $n_{\mathrm{NL}}^{\mathrm{eff}}$, as well as the changes in the value of the critical intensity where the effective nonlinear refractive index turns negative should be measurable.

The authors thank M. Kolesik for fruitful discussions. We acknowledge financial support through the AFOSR MURI "Mathematical Modeling and Experimental Validation of Ultrafast Nonlinear Light-Matter Coupling associated with Filamentation in Transparent Media", Grant No. FA9550-10-1-0561.

[1] P. Panagiotopoulos, P. Whalen, M. Kolesik, and J. V. Moloney, Nature Photonics **9**, 543 (2015).
[2] B. Shim, S. E. Schrauth, and A. L. Gaeta, Optics express **19**, 9118 (2011).
[3] D. Kartashov, S. Ališauskas, A. Pugžlys, A. Voronin, A. Zheltikov, M. Petrarca, P. Béjot, J. Kasparian, J.-P. Wolf, and A. Baltuška, Optics letters **37**, 3456 (2012).
[4] M. Cheng, A. Reynolds, H. Widgren, and M. Khalil, Optics letters **37**, 1787 (2012).
[5] Y. Nomura, H. Shirai, K. Ishii, N. Tsurumachi, A. A. Voronin, A. M. Zheltikov, and T. Fuji, Optics express **20**, 24741 (2012).
[6] D. Kartashov, S. Ališauskas, A. Pugžlys, A. Voronin, A. Zheltikov, M. Petrarca, P. Béjot, J. Kasparian, J.-P. Wolf, and A. Baltuška, Optics letters **38**, 3194 (2013).
[7] L. Bergé, J. Rolle, and C. Köhler, Physical Review A **88**, 023816 (2013).
[8] D. Bauer and P. Mulser, Phys. Rev. A **59**, 569 (1999).
[9] C. I. Blaga, F. Catoire, P. Colosimo, G. G. Paulus, H. G. Muller, P. Agostini, and L. F. DiMauro, Nature Physics **5**, 335 (2009).
[10] A. Becker and F. H. M. Faisal, Journal of Physics B: Atomic, Molecular and Optical Physics **38**, R1 (2005).
[11] L. V. Keldysh, Sov. Phys. JETP **20**, 1307 (1965).
[12] F. H. M. Faisal, Journal of Physics B: Atomic and Molecular Physics **6**, L89 (1973).
[13] H. R. Reiss, Phys. Rev. A **22**, 1786 (1980).
[14] D. Bauer, D. B. Milošević, and W. Becker, Phys. Rev. A **72**, 023415 (2005).
[15] S. V. Popruzhenko and D. Bauer, Journal of Modern Optics **55**, 2573 (2008).
[16] K. Schuh, J. Hader, J. Moloney, and S. Koch, J. Opt. Soc. Am. B **32**, 1442 (2015).
[17] A. Couairon and A. Mysyrowicz, Physics reports **441**, 47 (2007).
[18] J. Kasparian, M. Rodríguez, G. Méjean, J. Yu, E. Salmon, H. Wille, R. Bourayou, S. Frey, Y.-B. André, A. Mysyrowicz, R Sauerbrey, J.-P. Wolf, L. Wöste, Science **301**, 61 (2003).
[19] R. Alfano and S. Shapiro, Physical Review Letters **24**, 592 (1970).
[20] C. DAmico, A. Houard, M. Franco, B. Prade, A. Mysyrowicz, A. Couairon, and V. Tikhonchuk, Physical Review Letters **98**, 235002 (2007).
[21] C. Hauri, W. Kornelis, F. Helbing, A. Heinrich, A. Couairon, A. Mysyrowicz, J. Biegert, and U. Keller, Applied Physics B **79**, 673 (2004).
[22] J. Kasparian, R. Ackermann, Y.-B. André, G. Méchain, G. Méjean, B. Prade, P. Rohwetter, E. Salmon, K. Stelmaszczyk, J. Yu, A. Mysyrowicz, R Sauerbrey, L. Wöste, J.-P. Wolf, Optics express **16**, 5757 (2008).
[23] H. Haug and S. W. Koch, Quantum theory of the optical and electronic properties of semiconductors (World Scientific Publishing Company, 2004).
[24] W. Schäfer and M. Wegener, Semiconductor optics and transport phenomena (Springer, 2002).
[25] K. Schuh, J. Hader, J. Moloney, and S. Koch, Physical Review E **89**, 033103 (2014).
[26] J. Wahlstrand, Y.-H. Cheng, and H. Milchberg, Physical Review A **85**, 043820 (2012).
[27] D. Margoliash and W. Meath, The Journal of Chemical Physics **68**, 1426 (1978).
[28] H. Haug and A.-P. Jauho, Quantum Kinetics in Transport and Optics of Semiconductors, 2nd ed. (Springer-Verlag, Berlin, 2008).
[29] P. Lipavskỳ, V. Špička, and B. Velickỳ, Physical Review B **34**, 6933 (1986).
[30] L. J. Kieffer and G. H. Dunn, Reviews of Modern Physics **38**, 1 (1966).
[31] K. Schuh, M. Kolesik, E. Wright, and J. Moloney, Optics letters **39**, 5086 (2014).